Nanobiosensing (1)

DOI: 10.1002/anie.200902439

Nanostructuring of Patterned Microelectrodes To Enhance the Sensitivity of Electrochemical Nucleic Acids Detection**

Leyla Soleymani, Zhichao Fang, Xuping Sun, Hong Yang, Bradford J. Taft, Edward H. Sargent, and Shana O. Kelley**

Disease diagnosis on the basis of biomolecular analysis requires sensitive, cost-effective, and multiplexed assays.[1–3] Biomarker analysis based on electronic readout has long been cited as a promising approach that would enable the creation of a new family of chip-based devices with appropriate cost and sensitivity for medical testing.[4,5] The sensitivity of electronic readout, and specifically electrochemical analysis, is in principle sufficient to enable direct detection of small numbers of analyte molecules with simple instrumentation. Over the last several years, very high sensitivities have been demonstrated for nanomaterial-based electrochemical assays in particular,[6–9] whereby nanowire- and nanotube-based electrodes have shown some of the highest sensitivities to date. Whether these assays can be made practical and multiplexed remains to be seen, however, as the materials used have not been readily amenable to arrayed and straightforward fabrication.

Herein, we present a new system that enables nanostructured materials to be produced and used as nucleic acids sensors in an arrayed format. By using lithographically defined apertures as a template, we grew microelectrodes on a silicon chip by metal electrodeposition (Figure 1). Drawing upon the numerous studies of nanostructures with diverse morphologies generated as dispersions in solution,[10] we sought to manipulate precisely the surface morphology of these electrodes to control the level of nanostructuring present. We show that the production of nanostructured features on electrode surfaces is essential for the performance of the microelectrodes as ultrasensitive electrochemical detectors. A variety of studies have suggested that nanostructures are highly beneficial for biosensing applications because of the increased surface area, enhanced delivery of amplification agents, or precise biomolecule–electrode connections that are possible;[11–15] however, the role of nanostructuring in modulating biodetection sensitivity has not previously been addressed directly.

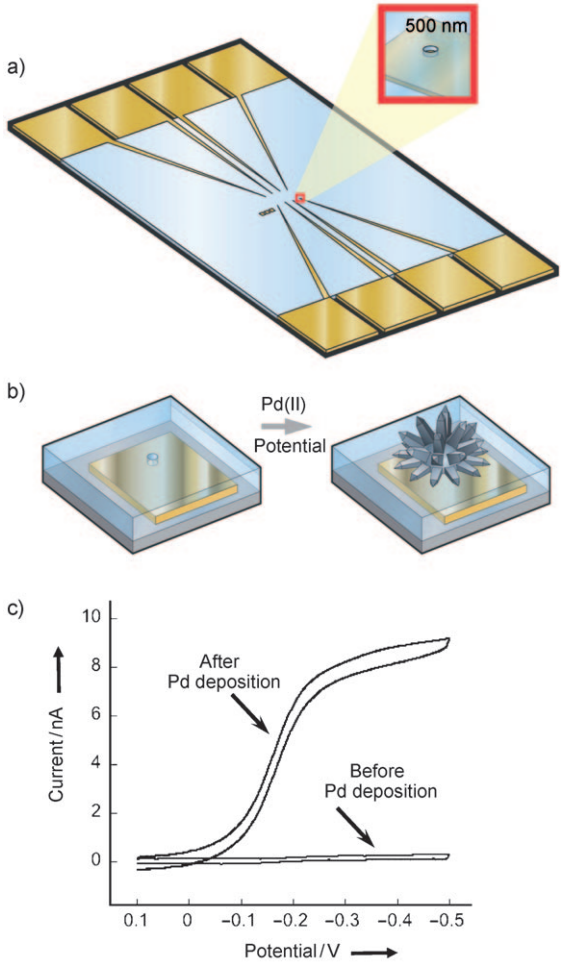

Figure 1. Fabrication of nanostructured microelectrodes on a silicon chip. a) Layout of the chip: A gold pattern is deposited on the chip surface with eight external contacts that are extended to narrow leads of a terminal width of 5 μm. A passivating layer of silicon dioxide is applied to the chip, and then apertures of 500 nm in diameter are opened at the end of each lead to provide a microelectrode template. b) Electrodeposition of microelectrodes: In the presence of a palladium salt and a supporting electrolyte, a potential is applied to each lead, and palladium electrodeposition is allowed to proceed until the microelectrode has reached the desired size. c) Cyclic voltammograms of $[Ru(NH_3)_6]^{3+}$ (3 mM) before and after Pd electrodeposition. The cyclic voltammograms show that the deposited structure behaves as a microelectrode.

We designed and fabricated a chip that would be amenable to the deposition of multiple independent sensing

[*] L. Soleymani, B. J. Taft, Prof. E. H. Sargent
Department of Electrical and Computer Engineering
University of Toronto
Toronto, ON M5S3G4 (Canada)
E-mail: ted.sargent@utoronto.ca
Z. Fang, X. Sun, H. Yang, Prof. S. O. Kelley
Department of Pharmaceutical Sciences and Department of Biochemistry, University of Toronto
Toronto, ON M5S3M2 (Canada)
E-mail: shana.kelley@utoronto.ca

[**] We acknowledge the support of the Ontario Centres of Excellence, Genome Canada through the Ontario Genomics Institute, the Ontario Ministry of Research and Innovation, and NSERC.

Supporting information for this article is available on the WWW under http://dx.doi.org/10.1002/anie.200902439.

elements in situ. Figure 1a shows an eightfold multiplexed chip. On a silicon substrate, an approximately 350 nm thick gold layer was patterned to connect eight 5 μm wide Au wires to large metal pads for connection to off-chip instrumentation. A pinhole-free insulating SiO_2 layer was deposited and patterned to create circular openings of approximately 500 nm in diameter at the end of each Au wire. This microfabricated chip formed the starting point for programmed bottom-up fabrication of the templated electrodes.

Owing to the versatility of metal electrodeposition for the generation of precisely defined structures on a variety of length scales,[16–20] we elected to use this process to generate our sensing electrodes. A particularly attractive feature of electrodeposition chemistry is that it can be used to create nanoscale features on microscale objects; this capacity has never been exploited in the generation of an electrochemical biosensing platform. We found that the electrodeposition of Pd into the half-micron openings in the insulating mask provided a means to generate microelectrodes that were remarkably reproducible (see the Supporting Information), robust, and highly programmable. These electrodes maximized current density and signal magnitude and thus exhibited ideal microelectrode behavior.

By searching parameter space for ways to manipulate the structural properties of the microelectrodes, we found that a wide range of morphologies could be accessed if the deposition time, applied potential, metal concentration, or electrolyte were varied. Our highest priority was to obtain structures with different degrees of nanostructuring, and we found that alteration of the applied potential and supporting electrolyte was the most effective way to reach this goal. When low potentials were used in combination with HCl as the supporting electrolyte, very smooth microelectrodes were generated (Figure 2a). When a higher potential was used (−100 mV) with $HClO_4$ as the electrolyte, microelectrodes with more extensive nanostructuring were produced (Figure 2b).

When different plating conditions were combined in sequence, composite structures were created that demonstrate the high degree of structural control possible with this approach. For example, a smooth sphere was generated with a low deposition potential (Figure 2c), and then a higher deposition potential was used in combination with a different electrolyte to "decorate" the smooth surface with nanostructures. The ability to generate such similar structures with nanostructuring as the only variable presents a unique opportunity to test the role of this property in biosensing directly and, potentially, to elucidate a parameter that could improve the sensing capabilities of electrochemical sensors to increase their relevance to the clinical diagnostics industry.

To use these sensors for nucleic acid detection, we applied an electrocatalytic reporter system previously developed by our research group.[6,7,21,22] Electrocatalysis provides electronic amplification, or gain, and thus facilitates high-sensitivity readout: hundreds of electrons can result from each biomolecular complexation event. The approach relies on the primary electron acceptor $[Ru(NH_3)_6]^{3+}$, which is attracted electrostatically to the electrode surfaces at levels that are correlated with the amount of bound nucleic acid.

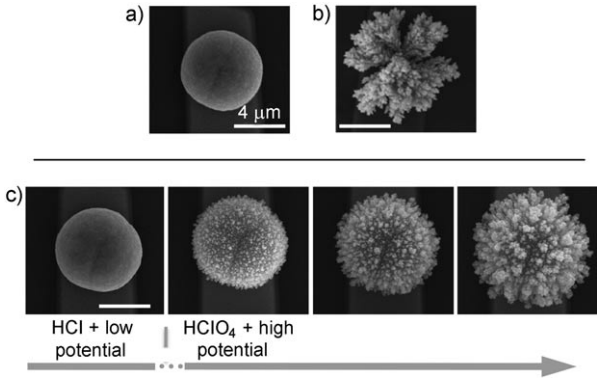

Figure 2. Control of palladium-microelectrode nanostructuring as visualized by scanning electron microscopy. a) Smooth Pd microelectrodes were generated by using a deposition potential of 0 mV and HCl as the supporting electrolyte with a plating time of 150 s. b) Highly nanostructured Pd microelectrodes were generated with a deposition potential of −100 mV and $HClO_4$ as the supporting electrolyte with a plating time of 40 s. c) Deposition of composite structures: The conditions used to generate the structure shown in (a) were first used to fabricate a smooth sphere. The plating solution was then changed, and the conditions used to generate the structure shown in (b) were then applied for 1 s, 2 s, and 5 s to systematically decorate the smooth sphere with nanostructures. The scale bar for all images is 4 μm.

The inclusion of $[Fe(CN)_6]^{3-}$ during electrochemical readout serves to regenerate the Ru^{III} substrate, as the Fe^{III} species is even easier to reduce; the Fe^{III} is repelled electrostatically from the electrode and thus primarily undergoes chemical reduction by Ru^{II} (though some direct electrochemical reduction of Fe^{III} is expected to occur). This assay was shown recently[6] to provide superior sensitivity when used in conjunction with probes made of peptide nucleic acids (PNAs),[23] which are charge neutral and therefore yield low background signals before the hybridization of a target sequence occurs. Microelectrodes were therefore modified with thiolated PNA probes and tested in hybridization assays.

We proceeded to investigate systematically the impact of nanostructuring on performance by varying microelectrode surface morphology and investigating nucleic acids detection sensitivity. We compared the performance of two different Pd microelectrodes with different surface structures in electrocatalytic nucleic acids detection (Figure 3). One microelectrode had a smooth hemispherical geometry, and the other had the same underlying structure with a layer of finely nanotextured structures (as shown in Figure 2b) generated through a two-step electrodeposition process. Thiolated PNA probes were immobilized on the electrodes, and the electrocatalytic reduction current was measured before and after hybridization with dilute (attomolar to picomolar) solutions of synthetic complementary DNA targets. Although both electrodes showed similar microelectrode behavior and limiting current magnitude (see graphs on the right in Figure 3), the nanostructured microelectrode showed superior sensitivity in the detection of DNA hybridization; for example, a strong signal change was observed with the nanostructured microelectrode, but not with the smooth microelectrode, in the presence of a target at a concentration of 10 fM (Figure 3).

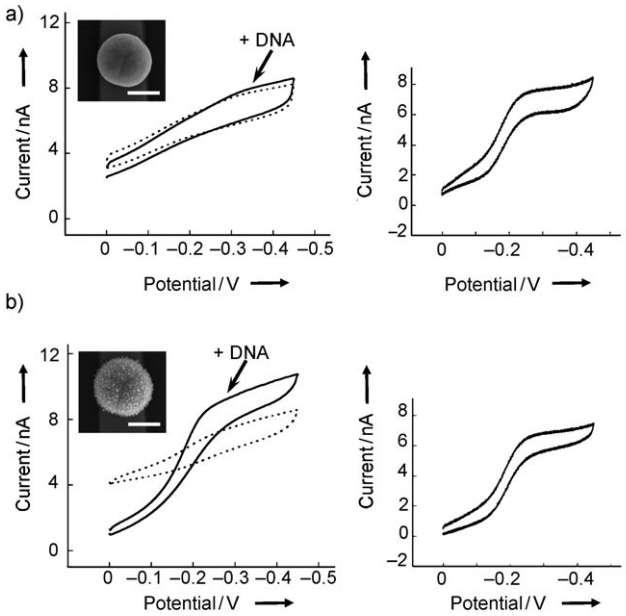

Figure 3. Comparison of the sensitivities of a) smooth and b) nanorough Pd microelectrodes. Signals observed before (dotted line) and after the incubation (solid line) of probe-modified microelectrodes with a synthetic target sequence (10 fM) for 60 min were compared by monitoring the limiting reductive current in a Ru^{III}/Fe^{III} electrocatalytic solution. The graphs on the right show representative cyclic voltammograms for each type of bare microelectrode in a solution containing $[Ru(NH_3)_6]^{3+}$ (3 mM). See the Supporting Information for experimental conditions, quantitation of the signal changes for multiple trials, and control experiments conducted with a noncomplementary sequence.

The limit of detection for this nanostructured microelectrode was estimated to be approximately 1 fM, whereas that for the smooth microelectrode was approximately 100 fM.

The importance of nanostructuring in the construction of biosensors with low detection limits is readily apparent in these experiments, which are the first in which this parameter has been analyzed directly in the context of biosensing applications. Macroelectrodes integrated with nanostructured Pd have been used previously to detect chemical species such as H_2O_2;[24] however, the use of patterned, nanostructured microelectrodes for the construction of sensitive biomolecular detectors has not been reported previously. It has been suggested previously that nanoscale sensing elements might be advantageous when their length scales approach those of biomolecular analytes.[7] To our knowledge, we have now tested this hypothesis directly for the first time.

Experimental Section

Chemicals and materials: Synthetic oligonucleotides were obtained from the Centre for Applied Genomics in the Hospital for Sick Children (Toronto, Canada). Thiolated PNA oligomers were obtained from Biosynthesis Inc.; 6-mercapto-1-hexanol (MCH, 97%), hexaammineruthenium chloride, potassium ferricyanide, magnesium chloride hexahydrate, and palladium(II) chloride(99.9+%) were purchased from Sigma–Aldrich Canada Ltd.; 70% perchloric acid, sulfuric acid, ACS-grade acetone, and isopropyl alcohol were obtained from EMD (USA); 6N hydrochloric acid was purchased from VWR (USA).

Chip fabrication: The chips were fabricated at the Canadian Photonics Fabrication Center. Three-inch silicon wafers were first passivated with a thick layer of thermally grown silicon dioxide. A 350 nm gold layer was then deposited on the chip by electron-beam-assisted gold evaporation. The gold film was patterned by standard photolithography and a lift-off process. A 500 nm layer of insulating silicon dioxide was deposited by chemical vapor deposition. Apertures of 500 nm in diameter were imprinted on the electrodes by standard photolithography, and 2×2 mm^2 bond pads were exposed by standard photolithography.

Fabrication of nanostructured microelectrodes: Chips were cleaned by rinsing sequentially with acetone, isopropyl alcohol, and deionized water for 30 s and dried with a flow of nitrogen. Electrodeposition was performed at room temperature with a Bioanalytical Systems Epsilon potentiostat with a three-electrode system featuring an Ag/AgCl reference electrode and a platinum-wire auxiliary electrode. Apertures (500 nm in diameter) on the fabricated electrodes were used as the working electrode and were contacted by using the exposed bond pads. $H_2[PdCl_4]$ was synthesized by treating palladium(II) chloride with hydrochloric acid. Electrodeposition was performed with $H_2[PdCl_4]$ (5 mM) in solution.

Preparation and purification of oligonucleotides: All synthetic oligonucleotides were purified stringently by reversed-phase HPLC. The following probe and target sequences were used in the experiments: PNA probe sequence 1: NH_2-Cys-Gly-ATA AGG CTT CCT GCC GCG CT-$CONH_2$, complementary target sequence: $^{5'}$AGC GCG GCA GGA AGC CTT AT$^{3'}$, noncomplementary target sequence: $^{5'}$TTT TTT TTT TTT TTT TTT TT$^{3'}$. Oligonucleotides were quantitated by measuring absorbance at 260 nm, and extinction coefficients were calculated by using the following website: http://www.idtdna.com/analyzer/Applications/OligoAnalyzer/.

Modification of nanostructured microelectrodes (NMEs) with PNA probes: A solution containing thiolated single-stranded PNA (500 nM), sodium phosphate (pH 7, 25 mM), and sodium chloride (25 mM) was heated at 50°C for 10 min. MCH (10 mM) was then added to a final MCH concentration of 100 nM. A portion of this mixture (0.5–10 μL) was deposited on the NMEs in a dark humidity chamber overnight at 4°C. The NMEs were rinsed in a sodium phosphate buffer (pH 7, 25 mM) containing NaCl (25 mM) before measurements.

Electrochemical measurements: Electrocatalytic signals were measured in solutions containing $[Ru(NH_3)_6]^{3+}$ (10 μM), sodium phosphate (pH 7, 25 mM), sodium chloride (25 mM), and $[Fe(CN)_6]^{3-}$ (4 mM) after degassing with nitrogen. Cyclic voltammetry signals before and after hybridization were collected with a scan rate of 100 mV s^{-1}. The limiting reductive current (I) was quantified by subtracting the background current at 0 mV from the cathodic current at −300 mV. Signal changes corresponding to hybridization were calculated according to the following equation: $\Delta I(\%) = 100\,(I_{ds} - I_{ss})/I_{ss}$ (ss = before hybridization, ds = after hybridization). Detection limits were approximated as the first concentration at which the signal, after subtraction of the background signal (noncomplementary ΔI), was at least three times higher than the standard deviation at that concentration.

Hybridization protocol: Hybridization solutions were typically solutions of the target sequences in sodium phosphate buffer (pH 7, 25 mM) containing NaCl (25 mM). Electrodes were incubated at 37°C in the dark in a humidity chamber for 60 min and were washed extensively with the buffer before electrochemical analysis. A solution volume of 10 μL was used for hybridization experiments.

Received: May 7, 2009
Revised: August 17, 2009
Published online: October 6, 2009

Keywords: biosensors · microchips · microelectrodes · nucleic acids · patterned nanostructures

[1] J. Bell, *Nature* **2004**, *429*, 453 – 456.
[2] D. R. Walt, *Science* **2005**, *308*, 217 – 219.
[3] A. D. Weston, L. Hood, *J. Proteome Res.* **2004**, *3*, 179 – 196.
[4] T. G. Drummond, M. G. Hill, J. K. Barton, *Nat. Biotechnol.* **2003**, *21*, 1192 – 1199.
[5] F. Ricci, K. W. Plaxco, *Microchim. Acta* **2008**, *163*, 149 – 155.
[6] Z. Fang, S. O. Kelley, *Anal. Chem.* **2009**, *81*, 612 – 617.
[7] R. Gasparac, B. J. Taft, M. A. Lapierre-Devlin, A. D. Lazareck, J. M. Xu, S. O. Kelley, *J. Am. Chem. Soc.* **2004**, *126*, 12270 – 12271.
[8] B. Munge, G. D. Liu, G. Collins, J. Wang, *Anal. Chem.* **2005**, *77*, 4662 – 4666.
[9] T. Selvaraju, J. Das, K. Jo, K. Kwon, C. Huh, T. K. Kim, H. Yang, *Langmuir* **2008**, *24*, 9883 – 9888.
[10] I. Willner, R. Baron, B. Willner, *Biosens. Bioelectron.* **2007**, *22*, 1841 – 1852.
[11] X. Yu, B. Munge, V. Patel, V. Jensen, G. Jensen, A. Bhirde, J. D. Gong, S. N. Kim, J. Gillespie, J. S. Gutkind, F. Papadimitrakopoulos, J. F. Rusling, *J. Am. Chem. Soc.* **2006**, *128*, 11199 – 11205.
[12] V. Mani, B. V. Chikkaveeraiah, V. Patel, J. S. Gutkind, J. F. Rusling, *ACS Nano* **2009**, *3*, 585 – 594.
[13] Y. Xiao, F. Patolsky, E. Katz, J. F. Hainfeld, I. Willner, *Science* **2003**, *299*, 1877 – 1881.
[14] R. Szamocki, S. Reculusa, S. Ravaine, P. N. Bartlett, A. Kuhn, R. Hempelmann, *Angew. Chem.* **2006**, *118*, 1340 – 1344; *Angew. Chem. Int. Ed.* **2006**, *45*, 1317 – 1321.
[15] C. Burda, X. Chen, R. Narayanan, M. A. El-Sayed, *Chem. Rev.* **2005**, *105*, 1025 – 1102.
[16] T. D. Clark, J. Tien, D. C. Duffy, K. E. Paul, G. M. Whitesides, *J. Am. Chem. Soc.* **2001**, *123*, 7677 – 7682.
[17] C. D. Keating, M. J. Natan, *Adv. Mater.* **2003**, *15*, 451 – 454.
[18] D. A. LaVan, P. M. George, R. Langer, *Angew. Chem.* **2003**, *115*, 1300 – 1303; *Angew. Chem. Int. Ed. Engl.* **2003**, *42*, 1262 – 1265.
[19] T. Kline, M. Tian, J. Wang, A. Sen, M. W. Chan, T. E. Mallouk, *Inorg. Chem.* **2006**, *45*, 7555 – 7565.
[20] M. Lahav, E. A. Weiss, Q. Xu, G. M. Whitesides, *Nano Lett.* **2006**, *6*, 2166 – 2171.
[21] M. A. Lapierre, M. M. O'Keefe, B. J. Taft, S. O. Kelley, *Anal. Chem.* **2003**, *75*, 6327 – 6333.
[22] M. A. Lapierre-Devlin, C. L. Asher, B. J. Taft, R. Gasparac, M. A. Roberts, S. O. Kelley, *Nano Lett.* **2005**, *5*, 1051 – 1055.
[23] M. Egholm, O. Buchardt, L. Christensen, C. Behrens, S. M. Freier, D. A. Driver, R. H. Berg, S. K. Kim, B. Norden, P. E. Nielsen, *Nature* **1993**, *365*, 566 – 568.
[24] P. Zhou, Z. Dai, M. Fang, X. Huang, J. Bao, *J. Phys. Chem. C* **2007**, *111*, 12609 – 12616.

